Excited superdeformed bands in ^{154}Dy and cranked relativistic mean field interpretation

Q. A. Ijaz, W. C. Ma, H. Abusara, A. V. Afanasjev, Y. B. Xu, R. B. Yadav, and Y. C. Zhang
Department of Physics and Astronomy, Mississippi State University, Mississippi State, Mississippi 39762, USA

M. P. Carpenter, R. V. F. Janssens, T. L. Khoo, T. Lauritsen, and D. T. Nisius
Physics Division, Argonne National Laboratory, Argonne, Illinois 60439, USA
(Received 31 July 2009; published 29 September 2009)

A Gammasphere experiment has been carried out using the ^{122}Sn(^{36}S,4n) reaction to search for excited superdeformed (SD) structures in ^{154}Dy to investigate the properties of neutron orbitals at superdeformation. Five new excited SD bands have been identified with intensities ranging from ∼0.7% to ∼0.03% relative to the ^{154}Dy reaction channel. Bands SD1, SD3, SD5, and SD6 are interpreted within the cranked relativistic mean field theory by using the effective alignment method. High-N intruder configurations are also discussed for bands SD2 and SD4, based on a comparison of their dynamic moments of inertia, which rise with increasing rotational frequency, with those of similar bands in neighboring nuclei.

DOI: 10.1103/PhysRevC.80.034322 PACS number(s): 21.10.Re, 21.60.−n, 23.20.Lv, 27.70.+q

I. INTRODUCTION

The properties of the excitations occurring in the superdeformed (SD) energy minimum continue to be a subject of current interest. In the $A \sim 150$ mass region of superdeformation, there is convincing evidence, accumulated over years of study, pointing to the role of single-particle degrees of freedom. Observables, such as the dynamic moments of inertia, $J^{(2)}$, [1–3], effective alignments $i_{\rm eff}$ [4,5], relative quadrupole moments [6], and the evolution of these physical quantities with rotational frequency, can be understood well in most cases in terms of the occupation of single-particle orbitals.

The ^{154}Dy isotope is located near the upper boundary of the $A \sim 140$–150 SD island. Five SD bands were observed in ^{153}Dy [7], but only single SD bands have been reported so far in ^{154}Dy [8] and ^{155}Dy [9]. A detailed study of the SD structures in ^{154}Dy will not only help explore the limits of this SD island and the evolution of the neutron orbitals at superdeformation but also aid in understanding the nature of excitations in the SD well. The transitional nucleus ^{154}Dy has a prolate shape at low spins. Prolate rotational bands terminate in the spin $40\hbar$–$50\hbar$ range [10]. Above the yrast line, a prolate-to-oblate phase transition has been identified through the investigation of quasi-continuum γ rays [11]. The structures along and above the yrast line are more collective in ^{154}Dy than in ^{152}Dy [12] and ^{153}Dy [13]. The SD band in ^{154}Dy was the first example of a SD band decaying at high spin to prolate collective states along the yrast line [8]. For all other cases in the $A = 150$ and $A = 190$ regions, the SD bands decay to normal deformed (ND) yrast levels, which correspond either to oblate aligned single-particle configurations (the $A = 150$ region) or to oblate weakly collective states (the $A = 190$ region). As a consequence, the feeding from SD states to the ND levels in ^{154}Dy spans a much broader spin range than in other SD nuclei. It is also worth mentioning that one of the excited bands in ^{152}Dy [14] has recently been connected to the yrast SD band [15]. Surprisingly, the measured properties of this excited band are consistent with an octupole vibration. In the mass $A \sim 190$ region, however, a number of excited SD bands in even-even nuclei have been interpreted in terms of collective excitations, in particular, octupole vibrations [16]. Therefore, a further study of SD bands in ^{154}Dy has the potential to reveal new excitation properties of the nucleus in the SD well.

The known SD band in ^{154}Dy was identified in an experiment with the Early Implementation version of Gammasphere, which consisted of only 36 germanium spectrometers [8]. We carried out a further study of ^{154}Dy with the full Gammasphere array. In this paper, we report on the discovery of five new excited SD bands in ^{154}Dy and on the study of their properties. The experimental details and results are presented in Secs. II and III, respectively; the theoretical analysis is discussed in Sec. IV.

II. EXPERIMENT AND DATA ANALYSIS PROCEDURES

Excited states in ^{154}Dy were populated via the ^{122}Sn(^{36}S,4n) reaction at a beam energy of 165 MeV. The experiment was performed at the 88-Inch Cyclotron of the Lawrence Berkeley National Laboratory. The target consisted of a stack of three 330 μg/cm^2 isotopically enriched, self-supporting foils. Decay γ rays were detected with the Gammasphere spectrometer array [17], which consisted of 103 Compton-suppressed Ge detectors. A total of 1.5×10^9 events was collected. Five or more suppressed Ge detectors were required to fire in prompt coincidence for an event to be recorded.

In the off-line analysis, the data were sorted into a database containing the γ-ray energies and detector identification for each event. The RADWARE software package [18] was used to construct three-dimensional (cube) and four-dimensional (hypercube) histograms and to analyze the γ-ray coincidence relationships. The RADWARE SD band search routine was used to find new bands. The statistics and quality of the present data set are significantly improved over that obtained with the Early Implementation version of Gammasphere [8]. A study of band termination in ^{154}Dy, using the new data set, has already been published [10].

III. EXPERIMENTAL RESULTS

Five new SD bands, labeled SD2 through SD6, have been identified in ^{154}Dy. The spectra of all six SD bands are presented in Fig. 1. Five known SD bands in ^{153}Dy [7] have also been observed in these data with intensities comparable to those of the SD bands in ^{154}Dy. Although the previously known SD1 band in ^{154}Dy has transition energies very similar to those of SD3 band in ^{153}Dy, SD2–SD5 are clearly different, except that five transitions in the SD3 band of ^{154}Dy have

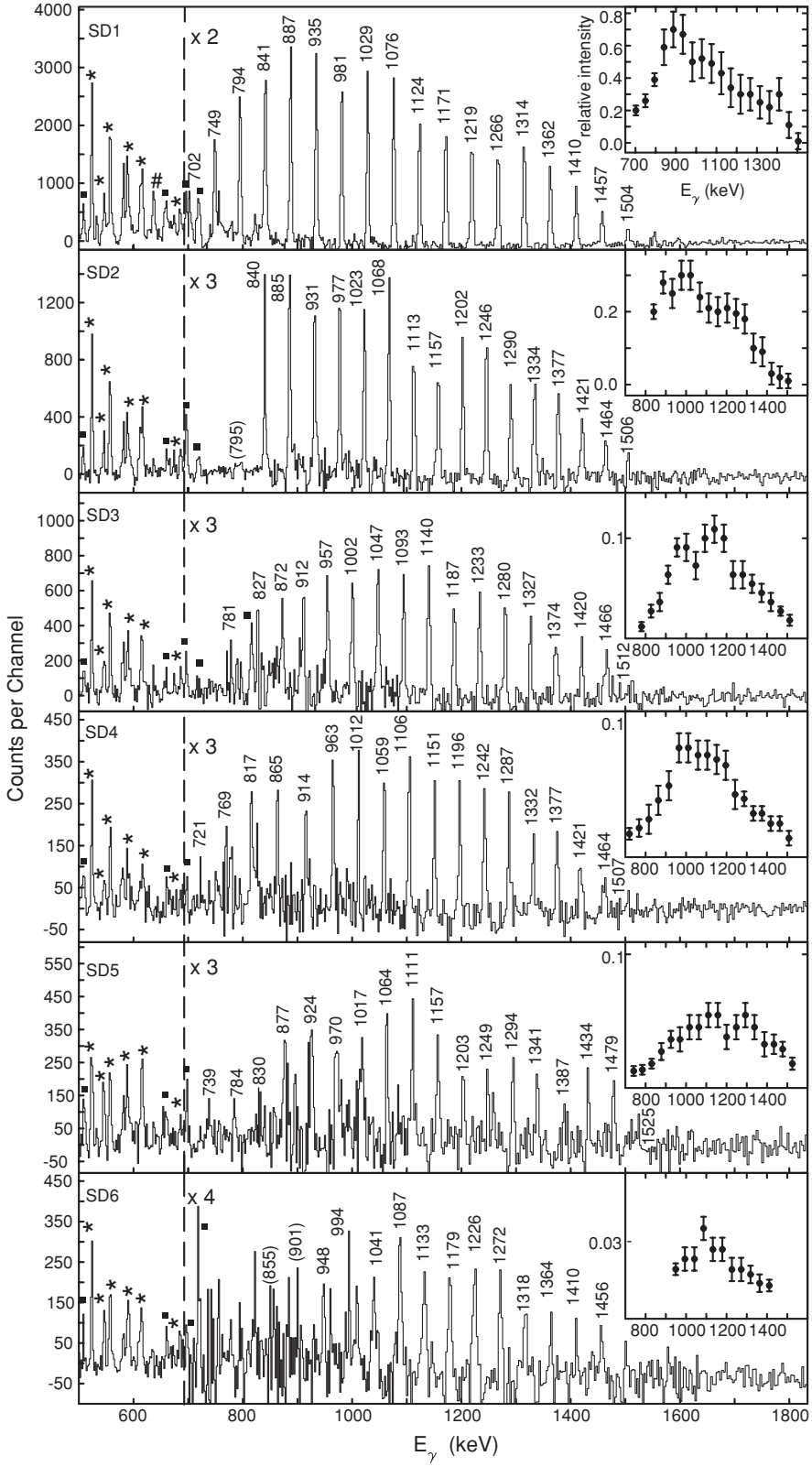

FIG. 1. Coincidence γ-ray spectra for bands SD1–SD6 in ^{154}Dy. The spectra were extracted from a four-fold coincidence histogram by summing all clean triple-gated spectra. The ND yrast transitions are marked with asterisks ($*$), and the transitions in the lowest negative-parity band are marked with filled squares. The symbol # in the SD1 spectrum denotes a 636-keV contamination from ^{153}Dy. The inset in each spectrum provides the intensity profile of the SD band.

γ-ray energies similar ($\leqslant$1.7 keV) to those of the SD4 band transitions in ^{153}Dy. However, SD6 band of ^{154}Dy is very similar to the SD1 band of ^{153}Dy. The differences of γ-ray energies between the two bands are $\leqslant$2.5 keV for seven transitions, and $\leqslant$4.4 keV for the remaining seven transitions, which provided some clean gates for the SD6 band. The assignment of new SD bands to ^{154}Dy has been carefully checked. It was possible to obtain clean coincidence spectra for all SD bands using the hypercube and to investigate their coincidence relationships with low-lying ND transitions in ^{154}Dy. The bands feed both the positive-parity ND yrast states and the lowest negative-parity ND band.

The new bands exhibit the typical characteristics of the SD bands in the $A \sim 150$ region. Thus, each band consists of long sequences (14–19) of transitions in coincidence with each other; the energy spacings between γ rays are approximately equal to 46 keV, which is similar to those of other SD bands in this mass region. For all bands the γ-ray intensity increases with decreasing transition energy until a constant value is reached and a decay-out occurs over a few transitions at the lowest energies. We estimate the intensities of bands SD1–SD6 relative to the strongest ND yrast transition in ^{154}Dy to be 0.70(10)%, 0.30(10)%, 0.11(5)%, 0.07(4)%, 0.05(3)%, and 0.03(2)%, respectively.

The lowest SD1 transition to carry 100% of the in-band intensity has an energy of 841 keV, and the decay-out of the band proceeds over four transitions (Fig. 1). The corresponding transition in the ^{152}Dy(1) band (denoting the ^{152}Dy Band 1 in Ref. [14]) is at 693 keV, and the decay-out of this band proceeds over only two transitions. This difference was attributed in Ref. [8] to a higher excitation energy above the yrast line in the ^{154}Dy case. The spectra of Fig. 1 further reveal that the energy of the lowest transition to carry the full intensity of each band gradually increases (from SD1 to SD6). The decay-out is seen to proceed over more and more transitions (except in SD6, where the lower spin transitions are too weak to identify). This may be caused by increasingly higher excitation energies of the SD bands.

IV. DISCUSSION AND THEORETICAL ANALYSIS

The theoretical interpretation of the observed bands was performed with the cranked relativistic mean field (CRMF) approach [3,4]. This approach has been successfully applied to the interpretation of different properties of SD bands in the $A \sim 150$ mass region [3,4], as well as to the study of rotational structures in different parts of the nuclear chart (see Ref. [19] and references therein). In the past, the interpretation of the single-particle structure of the majority of observed SD bands was performed by means of the effective alignment approach [4,5]. This approach is also used here. The effective alignment $i_{\rm eff}$ of two bands A and B, that is, the difference between their spins at constant rotational frequency $\hbar\omega$, is defined as [4,5]

$$i_{\rm eff}(\hbar\omega) = I_B(\hbar\omega) - I_A(\hbar\omega). \quad (1)$$

This quantity includes both the alignment of the single-particle orbital by which two compared bands differ and

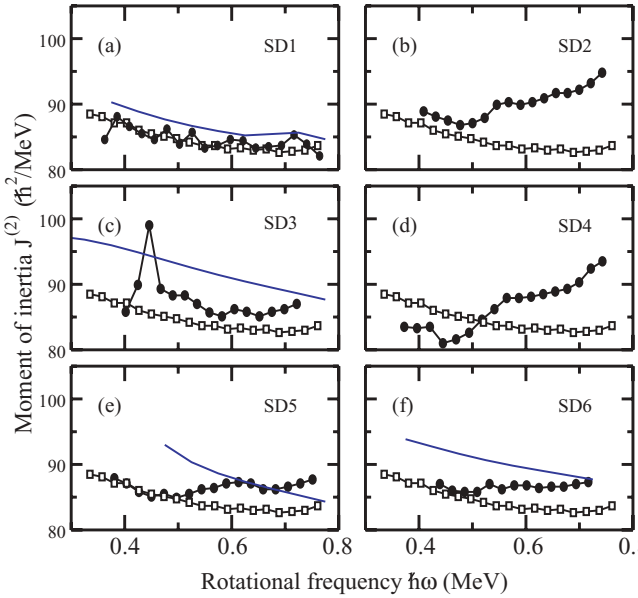

FIG. 2. (Color online) The dynamic moments of inertia $J^{(2)}$ of the six SD bands in ^{154}Dy compared with those calculated for the configurations assigned to these bands. Experimental values are shown by filled circles; the theoretical results correspond to the solid lines. The $J^{(2)}$ moment of the yrast SD band in ^{152}Dy is given by open circles.

the polarization effect associated with the occupation of this orbital. The spins are not known for the SD bands observed in ^{154}Dy; however, they are known for the yrast SD band in ^{152}Dy [20]. The latter serves as a reference band (band A) in the effective alignment method. Thus, by comparing calculated and experimental effective alignments in the pairs of the SD bands ^{152}Dy(1)/^{154}Dy(i) one can not only establish the structure of the SD bands in ^{154}Dy, but also suggest spins for these bands.

The pairing correlations are neglected in the CRMF calculations. As seen from systematic studies in this mass region, this is a fairly good approximation for rotational frequencies above $\hbar\omega \sim 0.5$ MeV [3–5]. The $J^{(2)}$ values of the SD1, SD3, and SD5 (up to the band crossing at $\hbar\omega \sim 0.53$ MeV) bands decrease with increasing rotational frequency (see Fig. 2). This is a feature typical for rotational bands with weak pairing [3] and justifies their interpretation within the CRMF formalism without pairing. The calculations are performed with the NL1 parametrization of the relativistic mean field (RMF) Lagrangian. The CRMF equations are solved in the basis of an anisotropic three-dimensional harmonic oscillator in Cartesian coordinates characterized by the deformation parameters $\beta_2 = 0.5$ and $\gamma = 0^\circ$ and the oscillator frequency $\hbar\omega_0 = 41A^{-1/3}$ MeV. The truncation of the basis is performed in such a way that all states belonging to the shells up to fermionic number $N_F = 14$ and bosonic number $N_B = 16$ are taken into account. Our numerical analysis indicates that this truncation scheme provides sufficient numerical accuracy for the physical quantities of interest.

All configurations in ^{154}Dy are labeled by the occupation of the two neutron orbitals above the $N = 86$ SD shell gap. This means that the ^{152}Dy yrast SD configuration $\pi 6^4 \nu 7^2$, in terms

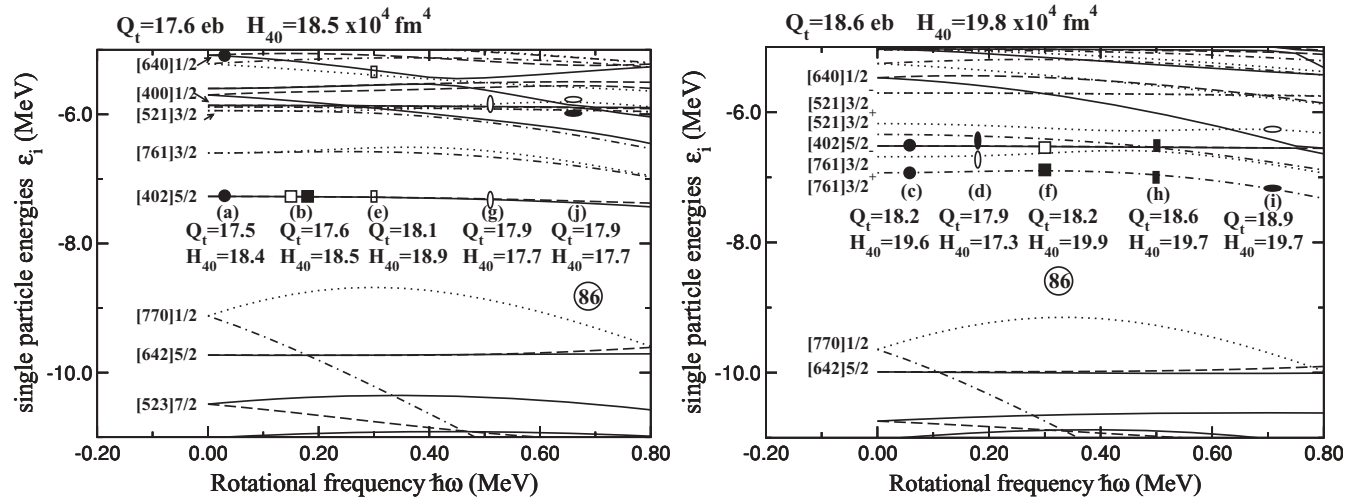

FIG. 3. (Left) Neutron single-particle energies (Routhians) in the self-consistent rotating potential as a function of the rotational frequency $\hbar\omega$. They are given along the deformation path of the yrast configuration in ^{154}Dy and obtained in the calculations with the NL1 parametrization of the RMF Lagrangian. Long-dashed, solid, dot-dashed, and dotted lines indicate $(\pi = +, r = +i)$, $(\pi = +, r = -i)$, $(\pi = -, r = +i)$, and $(\pi = -, r = -i)$ orbitals, respectively. At $\hbar\omega = 0.0$ MeV, the single-particle orbitals are labeled by the asymptotic quantum numbers $[Nn_z\Lambda]\Omega$ (Nilsson quantum numbers) of the dominant component of the wave function. The occupation of the neutron orbitals above the $N = 86$ SD shell gap is shown by open and solid symbols for the $r = -i$ and $r = +i$ orbitals, respectively. The configurations are labeled by the letters (a) through (j). Their transition quadrupole moments Q_t (in eb) and mass hexadecapole moments H_{40} (in units of 10^4 fm^4), at rotational frequency $\hbar\omega = 0.65$ MeV, are shown below the configuration labels. The values above the figure show the equilibrium Q_t and H_{40} moments at rotational frequency $\hbar\omega = 0.65$ MeV of the configuration for which the Routhian diagram is plotted. (Right) The same as the left panel, but for the $\nu[761]3/2^+ \otimes \nu[521]3/2^+$ configuration.

of the occupation of the intruder proton $N = 6$ and neutron $N = 7$ orbitals, serves as a reference for labeling ^{154}Dy configurations. All possible low-lying SD configurations, for which convergence has been achieved in the calculations, are included in the analysis, and their structures are shown in Fig. 3. The single-particle orbitals are labeled by $[Nn_z\Lambda]\Omega^{\text{sign}}$ where $[Nn_z\Lambda]\Omega$ are the asymptotic quantum numbers (Nilsson quantum numbers) of the dominant component of the wave function. The superscripts "sign" to the orbital labels are sometimes used to indicate the sign of the signature r for that specific orbital ($r = \pm i$).

Before performing a detailed theoretical analysis, it is important to understand the experimental features of the observed bands and to decide whether they agree with predictions based on the analysis of the SD bands in the neighboring nuclei ^{153}Dy and ^{155}Dy. This is because the lowest SD bands in these three nuclei are expected to be built on neutron single-particle orbitals located above the $N = 86$ SD shell gap (Fig. 3). The large $Z = 66$ SD shell gap makes proton excitations across this gap energetically unfavored in the frequently used parametrizations of the RMF Lagrangian (see, for example, Figs. 4, 11, and 12 in Ref. [4]). Only one neutron is located above the $N = 86$ SD shell gap in ^{153}Dy, allowing one to test the available single-neutron orbitals by comparing experimental and calculated effective alignments. Such a CRMF analysis has been performed in Ref. [4], where it is suggested that the SD1 band in ^{153}Dy is based on the $\nu[761]3/2^+$ orbital (see Fig. 5(a) in Ref. [4]) and the signature-degenerate bands SD2 and SD3 in ^{153}Dy are based on $\nu[402]5/2^+$ and $\nu[402]5/2^-$ orbitals, respectively (see Fig. 3(c) in Ref. [4]). This interpretation is in agreement with the one obtained in the framework of the cranked Nilsson-Strutinsky (CNS) approach [5,21]. Previous CRMF calculations did not give a consistent interpretation for the signature-degenerate SD4 and SD5 bands in ^{153}Dy within a pure single-particle picture, although the possibility of the occupation of the $\nu[514]9/2^{\pm}$ orbitals was considered in Ref. [4]. According to the cranked Woods-Saxon calculations of Ref. [7] and the CRMF calculations of Ref. [3], the $\nu[521]3/2$ orbital may be the neutron orbital associated with these bands. SD1 bands in ^{154}Dy and ^{155}Dy have been assigned the $(\nu[402]5/2)^2$ and $(\nu[402]5/2)^2 \otimes \nu[761]3/2^+)$ structures in Ref. [4], respectively. Under this configuration assignment, the lowest state in the SD1 band of ^{154}Dy has spin $I_0 = 24\hbar$. However, the comparison of the experimental and calculated effective alignments in the ^{152}Dy(1)/^{154}Dy(1) and ^{153}Dy(1,2)/^{155}Dy(1) pairs under these configuration assignments reveals a systematic discrepancy of about $0.5\hbar$ [4], which is somewhat larger than is normally seen.

Under these configuration assignments it is reasonable to expect that some of the excited SD bands in ^{154}Dy would originate from the occupation of the single $\nu[402]5/2$ orbital and of some other neutron orbital located above the $N = 86$ SD shell gap. This would lead to signature-degenerate SD bands from signature degeneracy for the $\nu[402]5/2^{\pm}$ orbitals. Indeed, the SD5 and SD6 bands in ^{154}Dy are interpreted as signature-degenerate bands based on these orbitals (see the

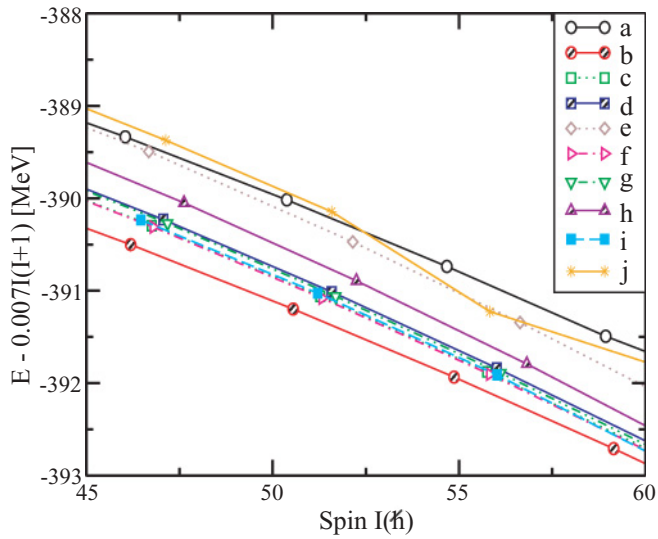

FIG. 4. (Color online) The energies of the calculated SD configurations in ^{154}Dy relative to a liquid drop reference $AI(I+1)$ with the inertia parameter $A = 0.007$. The structure of calculated configurations is given in Fig. 3.

following). A similar situation is expected if the excited SD bands are built on neutron orbitals active in either the SD4 or SD5 bands of ^{153}Dy and some other neutron orbital above the $N = 86$ SD shell gap, as the latter two ^{153}Dy SD bands are signature degenerate. However, no expected signature-degenerate partner band to the SD3 band in ^{154}Dy has been observed in the experiment.

The energies of the calculated configurations are presented in Fig. 4. The $(\nu[402]5/2)^2$ configuration (conf. b) is the lowest one in the calculations. The effective alignment in the ^{152}Dy(1)/^{154}Dy(1) pair is overestimated by $\sim 0.5\hbar$ in the calculations [Fig. 5(a)]. In comparison, the effective alignments in the ^{152}Dy(1)/^{153}Dy(2) and ^{152}Dy(1)/^{153}Dy(3) pairs, where the compared bands differ in the occupations of the $\nu[402]5/2^+$ and $\nu[402]5/2^-$ orbitals, is reproduced well in the calculations (see Fig. 3(a) in Ref. [4]). If the additivity principle for effective alignments [22,23] would hold, then $i_{\rm eff}$ in the pair ^{152}Dy(1)/^{154}Dy(1) would be close to zero above $\hbar\omega \sim 0.4$ MeV. This value is achieved in the calculations; however, the experimental value $i_{\rm eff} \sim -0.5\hbar$ for this pair of bands suggests that the additivity of effective alignments is violated in the data. Indeed, the effective alignment resulting from the $(\nu[402]5/2)^2$ configuration [Fig. 5(a)] is approximately equal to the sum of effective alignments from the $\nu[402]5/2^+$ and $\nu[402]5/2^-$ orbitals (as extracted from the comparison of the bands in ^{153}Dy and ^{152}Dy; see Fig. 3(a) in Ref. [4]).

The likely explanation of this experimental feature is related to the increase of pairing in the ^{154}Dy SD1 band as compared to SD1 in ^{152}Dy. The pairing in the yrast SD band in ^{152}Dy is considerably quenched because it is energetically expensive to scatter pairs of particles from the states below the large $N = 86$ and $Z = 66$ SD shell gaps to the levels above these gaps [24]. Although pairing is still present [2,24], it is weak. As a result, the calculations performed without pairing are successful in describing the properties of many SD bands [3–5,20] in this mass region. The addition of one neutron to the ^{152}Dy SD core, resulting in the ^{153}Dy SD bands, does not change the pairing since a single neutron above the $N = 86$ SD shell gap does not form a pair. This explains why the experimental data in ^{153}Dy are described well in the unpaired CRMF formalism [4]. The situation is changed when two neutrons are placed into two different signatures of the same Nilsson orbital above the $N = 86$ SD shell gap, as is the case in ^{154}Dy. The scattering of this neutron pair to other single-particle orbitals above the $N = 86$ SD shell gap is energetically inexpensive in view of the high density of the available single-particle states (see

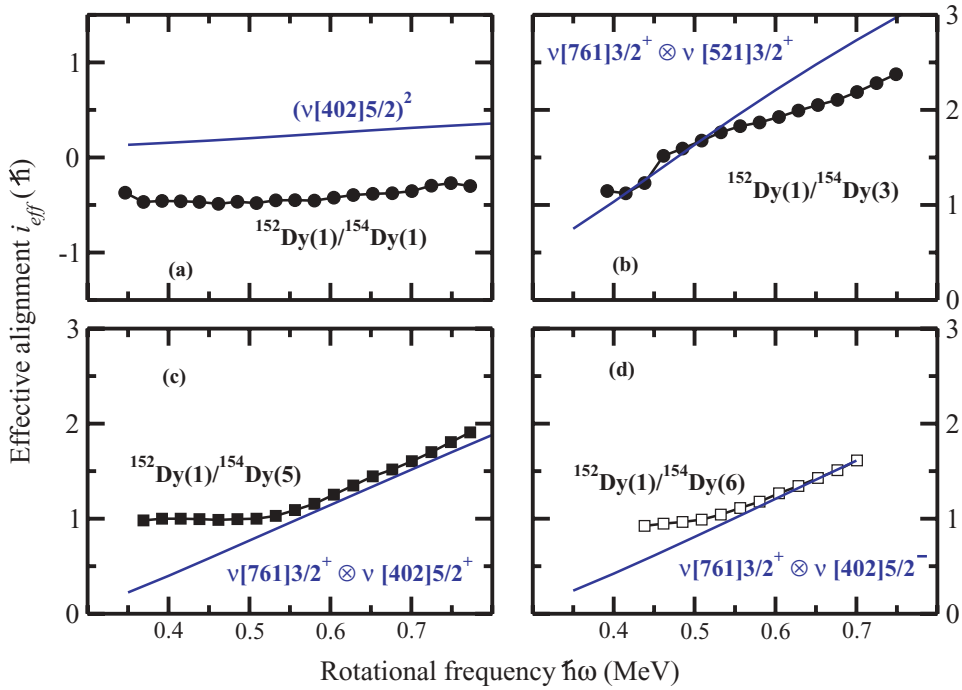

FIG. 5. (Color online) Effective alignments for the observed SD bands in ^{154}Dy and for the assigned configurations. Experimental values are shown by filled circles; the theoretical calculations are represented by solid lines. The yrast SD configuration (band) in ^{152}Dy is used as a reference so that the effective alignment measures the effect of two additional neutrons.

Fig. 3). Note that this density is also higher than the one below the $N = 86$ SD shell gap. This will result in increased neutron pairing for the $(\nu[402]5/2)^2$ configuration. In turn, this leads to a decrease in angular momentum at a given frequency and, thus, to negative values of the effective alignment $i_{\rm eff}$ for the ^{152}Dy(1)/^{154}Dy(1) pair. This mechanism, however, is not effective (owing to the broken pair) in configurations where two neutrons are placed in different Nilsson states above the $N = 86$ SD shell gap. It was pointed out in Ref. [1] that the behavior of $J^{(2)}$ moments with respect to $\hbar\omega$ is primarily influenced by the number of high-N intruder orbitals occupied in situations where the pairing is weak. The $J^{(2)}$ values of ^{154}Dy SD1 are essentially the same at all frequencies as those of SD1 in ^{152}Dy and of SD2 and SD3 in ^{153}Dy [7]. This is because these four bands, as just discussed, have the same high-N intruder configuration, $\pi 6^4 \nu 7^2$. As is seen in Fig. 2(a), the dynamic moment of inertia of the SD1 band is described rather well by the calculations.

The SD3 band undergoes a band crossing at $\hbar\omega \sim 0.45$ MeV [Fig. 2(b)], above which it exhibits a rather smooth behavior, as follows from the effective alignments $i_{\rm eff}$ [Fig. 5(b)] and the dynamic moments of inertia [Fig. 2(b)]. The $J^{(2)}$ values of this band are markedly higher than those seen in ^{152}Dy(1) band, but they are very similar to those seen in the ^{153}Dy SD1 band, where an additional $j_{15/2}$ orbital is believed to be occupied [4,25]. The analysis of the effective alignments [Fig. 5(b)] suggests that the SD3 band has the $\nu[761]3/2^+ \otimes \nu[521]3/2^+$ structure above the band crossing. Under this configuration assignment the lowest state in the band has spin $I_0 = 33\hbar$. The experimental effective alignment is reproduced well around $\hbar\omega \sim 0.5$ MeV, but it is overestimated by $0.5\hbar$ at the highest frequencies observed. This is, however, the typical accuracy for the description of effective alignments of the high-N intruder orbitals (see Ref. [4]). The experimental dynamic moment of inertia is also slightly overestimated in the calculations [Fig. 2(b)]. The calculations suggest that band SD3 should have a signature partner band with the $\nu[761]3/2^+ \otimes \nu[521]3/2^-$ structure. As follows from Fig. 3 (right panel), these two bands should be almost signature degenerate because of very small signature splitting of the $\nu[521]3/2^{\pm}$ orbitals at rotational frequency $\hbar\omega \geqslant 0.5$ MeV. However, no such band has been seen in experiment. This could be because the band population is at the very limit of experimental sensitivity.

The SD5 band undergoes a band crossing at $\hbar\omega \sim 0.55$ MeV [Fig. 2(e) and Fig. 5(c)]. Above this crossing, the effective alignment $i_{\rm eff}$ and dynamic moment of inertia are described very well by the $\nu[761]3/2^+ \otimes \nu[402]5/2^+$ configuration. Under this assignment, the lowest state in this band has spin $I_0 = 31\hbar$. The $J^{(2)}$ values are similar to those of the ^{152}Dy(1) band at frequencies lower than $\hbar\omega = 0.53$ MeV, but they increase compared to the latter above the crossing. This suggests that a strong interaction of some $\nu N = 5^+$ (where we label the orbital only by its principal quantum number N and the sign of the signature) and $\nu[761]3/2^+$ orbitals may be responsible for this band crossing and that the SD5 band does not contain a $\nu[761]3/2^+$ neutron below the crossing.

The SD6 band is the signature partner of SD5. This is supported by a comparison of effective alignments of the two bands, which indicates that the bands are signature degenerate [Figs. 5(c) and 5(d)]. The $\nu[761]3/2^+ \otimes \nu[402]5/2^-$ structure is assigned to the SD6 band. Under this configuration assignment, the effective alignment $i_{\rm eff}$ is very well described [Fig. 5(d)] and the dynamic moment of inertia is reasonably described [Fig. 2(f)] above the band crossing. The effective alignment analysis suggests that the lowest state in this band has spin $I_0 = 36\hbar$. The effective alignments from the $\nu[402]5/2^{\pm}$ and $\nu[761]3/2^+$ orbitals in ^{153}Dy are well described in the CRMF calculations (see Figs. 3(c) and 5(a) in Ref. [4]). Furthermore, the effective alignments from combined $\nu[761]3/2^+ \otimes \nu[402]5/2^{\pm}$ configurations in ^{154}Dy [Figs. 5(c) and 5(d)] are very close to the sum of effective alignments from individual $\nu[402]5/2^{\pm}$ and $\nu[761]3/2^+$ orbitals that were seen in ^{153}Dy. The experimental effective alignments of these bands with respect to the ^{152}Dy(1) band are also described well in the calculations for rotational frequency $\hbar\omega \geqslant 0.5$ MeV. Thus, the additivity of effective alignments is fulfilled in the case of bands SD5 and SD6. This is contrary to the case of the SD1 band in ^{154}Dy (see earlier discussion), where the violation of additivity of effective alignments is most likely due to the increase of neutron pairing in the SD1 band of ^{154}Dy as compared to the SD1 band in ^{152}Dy. This increase is not present in bands SD5 and SD6 since their configurations do not involve a neutron pair above the $N = 86$ SD shell gap. This is, most likely, the reason why the effective alignments in the ^{152}Dy(1)/^{154}Dy(5,6) pairs are described well in the calculations.

The $J^{(2)}$ values of the SD2 and SD4 bands exhibit a very different trend than those just discussed (see Fig. 6). The shape of these $J^{(2)}$ curves allows one to suggest a possible scenario for structure changes. The moments of these two bands decrease gradually with increasing rotational frequency up to $\hbar\omega \sim 0.5$ MeV. This type of behavior is typical for configurations in which the pairing is weak. By considering the relative properties of dynamic moments of inertia of these two bands with respect to that of the ^{152}Dy(1) band (see

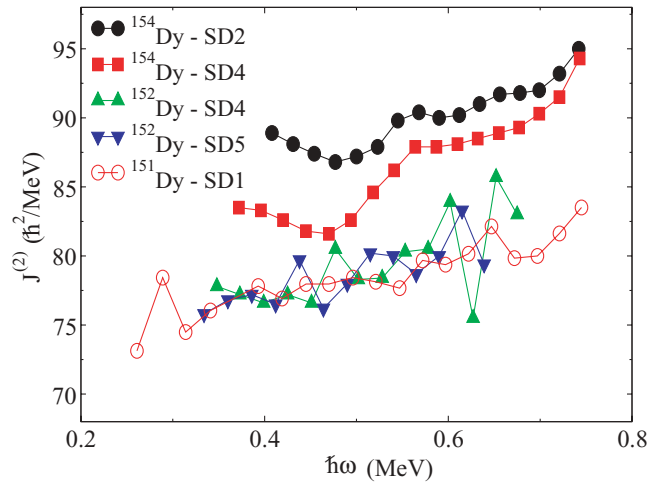

FIG. 6. (Color online) The $J^{(2)}$ moments of inertia rise vs rotational frequency for several SD bands in ^{151}Dy [26], ^{152}Dy [14], and ^{154}Dy.

Fig. 2), it is reasonable to suggest that the SD4 (SD2) band has less (more) intruder orbitals occupied than the SD1 band in ^{152}Dy at these frequencies. The dynamic moments of inertia increase considerably with increasing rotational frequency in the $\hbar\omega = 0.5$–0.6 MeV range. Unpaired band crossings resulting from a strong interaction of two orbitals with the same quantum numbers is a possible source for this feature. The fact that the band crossing in the SD2 and SD4 bands takes place in the same frequency suggests that the same pair of orbitals is involved in both instances. Above this crossing, the rate of increase in $J^{(2)}$ with $\hbar\omega$ is very similar to the one seen in the ^{152}Dy SD4 and SD5 bands [14] and in the ^{151}Dy SD1 band [26]. This increase quite likely indicates the rise of pairing correlations above the band crossing. As shown in Ref. [3], for the example of the ^{151}Dy SD1 band, it is unlikely that unpaired CRMF calculations can reproduce this trend in $J^{(2)}$. Calculations based on the CNS approach [5], another type of unpaired formalism, face the same problem [27]. Band crossings are also seen at the highest observed frequencies in the SD2 and SD4 bands of ^{154}Dy (Fig. 6). There might also be one additional crossing in the SD2 band at $\hbar\omega \sim 0.65$ MeV. Experience tells us that the calculations of such structures are quite complicated and seldom lead to a reliable interpretation in the unpaired formalism. Therefore, a detailed interpretation of the structure of bands SD2 and SD4 will not be attempted here. Nevertheless, the properties of the SD2 and SD4 bands above $\hbar\omega \sim 0.6$ MeV suggest that they have more intruder orbitals occupied than the configuration $\pi 6^4 \nu 7^2$ assigned to the SD1 band in ^{152}Dy.

V. SUMMARY

Five new excited SD bands have been observed in ^{154}Dy. The bands SD1, SD3, SD5, and SD6 were interpreted within the cranked relativistic mean field theory. The high-N intruder configuration $\pi 6^4 \nu 7^2$ was suggested for SD1 band, and $\pi 6^4 \nu 7^3$ was suggested for SD3, SD5, and SD6 at frequencies above $\hbar\omega \sim 0.5$ MeV. The rise of $J^{(2)}$ moments with increasing rotational frequency, seen in bands SD2 and SD4, may indicate the presence of pairing and of band crossings. Those features cannot be addressed in the current calculations within the unpaired formalism.

ACKNOWLEDGMENTS

This work was supported by the US Department of Energy, Office of Nuclear Physics, under Grant Nos. DE-FG02-95ER40939, DE-FG02-07ER41459 (MSU), and DE-AC02-06CH11357 (ANL).

[1] T. Bengtsson, I. Ragnarsson, and S. Åberg, Phys. Lett. **B208**, 39 (1988).
[2] W. Nazarewicz, R. Wyss, and A. Johnson, Nucl. Phys. **A503**, 285 (1989).
[3] A. V. Afanasjev, J. König, and P. Ring, Nucl. Phys. **A608**, 107 (1996).
[4] A. V. Afanasjev, G. A. Lalazissis, and P. Ring, Nucl. Phys. **A634**, 395 (1998).
[5] I. Ragnarsson, Nucl. Phys. **A557**, 167c (1993).
[6] W. Satula, J. Dobaczewski, J. Dudek, and W. Nazarewicz, Phys. Rev. Lett. **77**, 5182 (1996).
[7] B. Cederwall *et al.*, Phys. Lett. **B346**, 244 (1995).
[8] D. Nisius *et al.*, Phys. Rev. C **51**, R1061 (1995).
[9] S. M. Fischer *et al.*, Phys. Rev. C **54**, R2806 (1996).
[10] W. C. Ma *et al.*, Phys. Rev. C **65**, 034312 (2002).
[11] W. C. Ma *et al.*, Phys. Rev. Lett. **84**, 5967 (2000).
[12] T. L. Khoo *et al.*, Phys. Rev. Lett. **41**, 1027 (1978).
[13] M. Kortelahti *et al.*, Phys. Lett. **B131**, 305 (1983).
[14] P. J. Dagnall *et al.*, Phys. Lett. **B335**, 313 (1994).
[15] T. Lauritsen *et al.*, Phys. Rev. Lett. **89**, 282501 (2002).
[16] R. V. F. Janssens and T. L. Khoo, Annu. Rev. Nucl. Part. Sci. **41**, 321 (1991).
[17] I.-Y. Lee, Nucl. Phys. **A520**, 641c (1990).
[18] D. C. Radford, Nucl. Instrum. Methods Phys. Res. A **361**, 297 (1995).
[19] A. V. Afanasjev and H. Abusara, Phys. Rev. C **78**, 014315 (2008).
[20] T. Lauritsen *et al.*, Phys. Rev. Lett. **88**, 042501 (2002).
[21] G. de France *et al.*, Phys. Lett. **B331**, 290 (1994).
[22] I. Ragnarsson, Phys. Lett. **B264**, 5 (1991).
[23] M. Matev, A. V. Afanasjev, J. Dobaczewski, G. A. Lalazissis, and W. Nazarewicz, Phys. Rev. C **76**, 034304 (2007).
[24] Y. R. Shimizu *et al.*, Rev. Mod. Phys. **61**, 131 (1989).
[25] J. K. Johansson *et al.*, Phys. Rev. Lett. **63**, 2200 (1989).
[26] G. E. Rathke *et al.*, Phys. Lett. **B209**, 177 (1988).
[27] I. Ragnarsson (private communication, 2009).